Comparison of the Behaviour of an Al-Fe-Ce Alloy by Powder Metallurgy and by PBF-LB/M

J. Jpn. Soc. Powder Powder Metallurgy, **72** (2025) S1093-S1098
https://doi.org/10.2497/jjspm.16B-T6-30

Comparison of the Behaviour of an Al-Fe-Ce Alloy by Powder Metallurgy and by PBF-LB/M

Nicolò ARCIERI[1*], Diego MANFREDI[1,2] and Marco ACTIS GRANDE[3]

[1]Department of Applied Science and Technology (DISAT), Politecnico di Torino, Corso Duca degli Abruzzi 24, Turin, 10129, Italy.
[2]Istituto Italiano di Tecnologia (IIT), Center for Sustainable Future Technologies CSFT@Polito, Via Livorno 60, Turin, 10144, Italy.
[3]Department of Applied Science and Technology (DISAT), Politecnico di Torino, Viale T. Michel 5, Alessandria, 15121, Italy.

Abstract
Al-8Fe-4Ce is an aluminium alloy developed in the 80's as potential replacement for titanium in structural applications at medium service temperatures (up to 350 °C). This alloy was specifically tailored for powder metallurgy process since both the Fe and the Ce contents are far beyond the equilibrium solid solubility. Indeed, these elements are fundamental for the mechanical properties at high temperature. Nowadays, the study of Al alloys that can withstand service temperatures higher than 200 °C has regained momentum due to the emergence of additive manufacturing (AM) as reliable manufacturing processes. Among them, laser powder bed fusion for metals (PBF-LB/M) guarantees similar cooling rates of traditional rapid solidification techniques but with the ability to produce components with a high degree of complexity. In this study, Al-8Fe-4Ce was processed by press and sinter (P/S) and by PBF-LB/M and then the obtained samples were compared in terms of microstructure and mechanical properties.

Keywords: Aluminum alloy, Press and Sinter, PBF-LB/M

Introduction

Aluminum alloys are employed as structural materials thanks to their good specific mechanical properties, corrosion resistance and lightweight. 2xxx series (Al-Cu based system) and 7xxx series (Al-Zn based system) alloys are widely used to produce structural components for aerospace applications due to their outstanding mechanical properties[1,2)]. However, even these alloys cannot be used when service temperatures exceed 200 °C, due to the strengthening loss caused by the coarsening of the precipitates[3,4)]. Therefore, titanium-based alloys, steels and other heavier metals must be used between 200 °C and 450 °C, even though these materials are overdesigned for the aforementioned temperature range[3-5)].
For this reason, new high strength Al-alloys that can withstand service temperatures up to 450 °C have been intensively studied in the last few decades employing a combination of rapid solidification (RS) and powder metallurgy (PM)[6-9)]. Most of them contain transitional metals (TMs) such as iron, nickel, and chromium and rare earth elements (REEs). Iron and other TMs are traditionally considered harmful elements in cast and wrought Al alloys because of the detrimental formation of acicular phases[10)]. However, TMs and REEs are often added as alloying elements in RS Al alloys due to their low solid diffusion coefficient in the aluminum matrix and the high thermal stability of their precipitates[6)].
Many heat-resistant alloys based on the Al-TM-REE system have been developed including Al-8Fe-4Ce[11)]. This alloy was originally investigated as potential replacement of Ti-alloys in aerospace and defense applications, demonstrating high thermal stability at temperatures up to 350°C. Al-Fe-Ce based alloys were designed to take full advantage of the RS resulting from the gas-atomization and the following powder compaction. Indeed, the powder is consolidated by cold pressing, vacuum hot pressing, and then the resulting billet undergoes hot working[12)]. The outstanding mechanical properties of Al-Fe-Ce based alloys are mainly due to the high volume of thermally stable precipitates (up to 35 % in volume)[13)].
However, this manufacturing route requires several steps increasing the lead time and the cost of the final component. In addition, only simple geometries can be produced, limiting the use of this material.
Other manufacturing routes have been explored to process Al-8Fe-4Ce. For instance, Fass et al.[14)] investigated the phase stability up to 500 °C for melt spinned Al-8Fe-4Ce.
Press and sinter (P/S) could be an interesting alternative to the traditional route, since it is able to produce neat net shape objects saving time and energy. In this case, the powder is consolidated in a die with the shape of the final component then, if a biding is used, the green component is subjected to debiding and finally sintered[15)]. P/S aluminum alloys are commonly used in automotive sector for high volume components[16)].
Nowadays, additive manufacturing (AM) processes have been established as a reliable way to obtain metal components of complex shape starting from computer-aided design (CAD) files[17,18)]. Moreover, AM manufacturing technologies can help to reduce the waste of raw materials since they are not subtractive processes. Among the AM technologies, laser powder bed fusion for metals (PBF-LB/M) is the main route used to process Al alloys[18)]. However, only a few Al alloys are commercially available for PBF-LB/M. Most of them are based on cast Al-Si alloys due to their good processability but this kind of alloys cannot be used at high temperatures due to the quick drop in the mechanical response[3)]. On the other hand, other alloys contain rare and costly elements such as scandium, which drastically increased the cost of the material, making it suitable only for niche applications[18)]. Therefore, the research is pushing towards compositions that have high thermal stability and rely on abundant and cheaper alloying elements. New PBF-LB/M Al alloys have recently developed with this goal, containing TMs such as Fe, Cr and Mn[3)]. These alloys aim to take advantage of the rapid cooling (10^3-10^6 K/s) characteristic of PBF-LB/M to increase the solubility of TMs in the Al matrix and improve the mechanical properties[18)].
However, the investigation of totally new composition is time-consuming and expensive. Only a few studies, such as Sun et al.[19)] and Yu et al.[20)], have tried to investigate whether alloys already developed for other RS processes could be also manufactured by PBF-LB/M and how

*corresponding author, e-mail: nicolo.arcieri@polito.it

the microstructure and properties might be affected. The possible feasibility in using existing alloys coming from other RS processes will expand the available compositions on the market helping the widespread of this technology. Nowadays, AM Al-Fe and Al-Ce based alloys are gaining momentum due to environmental and economic reasons[10)]. Indeed, Al scraps often contains iron impurities that make it difficult to recycle for casting and wrought based products due to the detrimental effects on the mechanical properties of Al-Fe precipitates produced by the processing conditions. Therefore, the development of AM Al alloys with high contents of iron would be beneficial for the upcycling of Al scraps. In addition, iron is an abundant and low-cost alloying element. Likewise, cerium is considered an unexpensive alloying element being the most abundant REE. Cerium is also a byproduct of more valuable REEs extraction and is often discarded due to limited industrial applications[10,21)].
To summarize these considerations, the main goal of this study is the investigation and the comparison of the microstructure and the microhardness of Al-8Fe-4Ce alloy processed by two different promising PM routes: PBF-LB/M and P/S processes.

Experiment
In this study, the aluminum powder was purchased from Valimet (Stockton, CA). The nominal chemical composition of the alloy is reported in table 1.

Table 1. Nominal composition of Al-8Fe-4Ce.

Al	Fe	Ce	Si	Mn	Ti	Zn
Bal.	7.3-9.3	3.5-4.5	<0.2	<0.05	<0.05	<0.05

The particle size distribution (PSD) was evaluated with a laser granulometry Mastersizer 3000 analyser. PBF-LB/M powder was characterized by a PSD between 23 µm and 66 µm while P/S powder by a PSD centered to coarser values (D_{50} equal to 94 µm). Field emission scanning electron microscope (FE-SEM) Zeiss Supra TM 40 was used to investigate the morphology of the two powder batches. As can be seen in Fig. 1, both powders show a quasi-spherical shape, with the presence of some satellites.

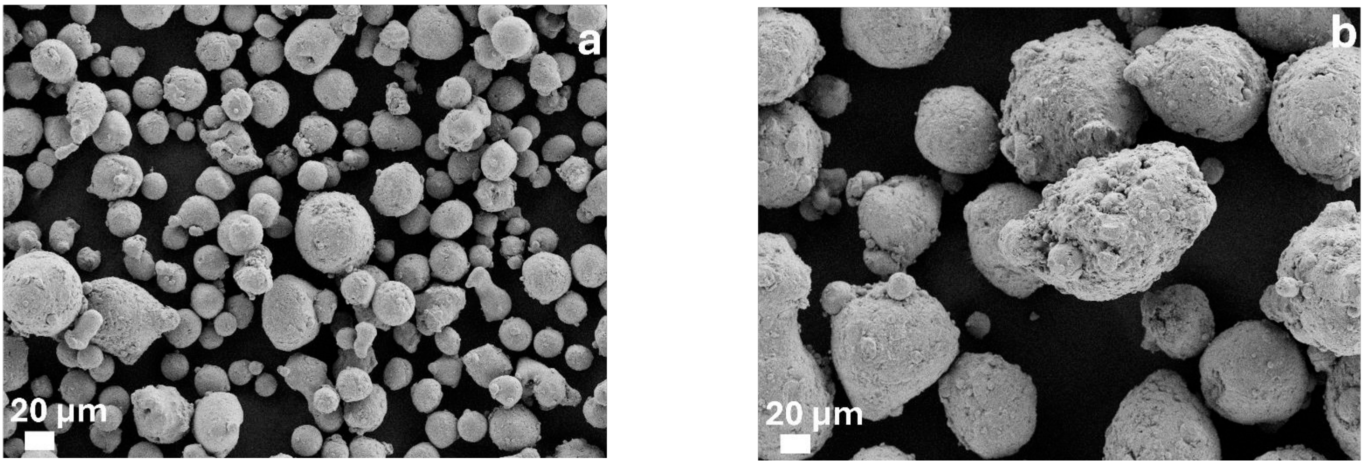

Fig.1 FE-SEM powder images (secondary electron detector). a) PBF-LB/M powder. b) P/S powder.

PBF-LB/M powder was processed using a Print Sharp 250 under argon atmosphere. The machine was equipped with a 500 W Yb fiber laser (spot size of 100 µm). The building platform was preheated at 150 °C to reduce the occurrence of delamination during the job. 10 x 10 x 10.5 mm^3 cubes were produced with different parameter combinations to assess the processability window of the alloy. Finally, the samples were separated from the platform using a wire electric discharge machine (W-EDM) Baoma BMW-3000.
P/S samples were produced by using a hydraulic press applying a pressure of 300 MPa (no biding was required). Then, the samples were sintered at 600 °C for 1h in nitrogen atmosphere in a TAV Minijet furnace with a heating rate of 10 °C/min. Green P/S samples had 55 x 10 x 10 mm^3 size.
Both PBF-LB/M and P/S samples were cut and then polished starting from grinding paper to silica suspension in order to obtain a mirror-like surface for the metallographic characterization. Density was evaluated by microscopy. Images for density evaluation were acquired using an optical microscope (OM) Leica DMI 5000 M. For each sample, 20 micrographs at 100X were acquired and then analyzed with ImageJ software. The mean level of the density was obtained by averaging the results obtained from all the micrographs. A tabletop SEM Phenom ProX was used to investigate the microstructure of the samples processed by PBF-LB/M and P/S routes. The tabletop SEM was operating at an accelerating voltage of 15 kV. Vickers microhardness tests were performed by using a HNVS-1000DX hardness tester. For each sample, micro indentations were carried out applying a static load of 0.5 kg and a dwell time of 10 s. Five indentations for each sample were considered according to ASTM E10-18 standard.

Results and Discussion

PBF-LB/M samples showed a relative density higher than 96%, with the best combination of parameters providing a relative density of 99.6% (see Fig. 2a). All samples were crack free except for those with a volumetric energy density (VED) lower than 55 J/mm^3. Crack formation in low VED samples is likely due to suboptimal liquid backfill, as reported by Shang et al.[22)] for a custom high-strength Al alloy. Fig. 2a reports an OM image of an unetched PBF-LB/M specimen. As can be seen, melt pools can be clearly recognized even without etching. On the other hand, P/S samples were not yet fully densified even after sintering at high temperature, even though the samples shown a significant dimensional shrinkage. The average relative density of the specimens was 93.54%. Indeed, the profile of the particles can still be recognized in some areas, as shown in Fig. 2b. This indicates that the use of a nitrogen atmosphere, combined with high temperature, is probably not enough to have a complete breakup of the Al_2O_3 layer that covers the particles. A possible solution to overcome this issue could be the addition of magnesium as sintering aid[15,23,24)]. In addition, magnesium could be beneficial to the mechanical properties as it increases the solid solution strengthening in Al alloys[1,24)].

Microhardness measurements for PBF-LBF samples gave an average value of 179.7 HV0.5 in the as built condition. This hardness value is close to the values of Scamalloy© and higher than AlSi10Mg[25)]. The high hardness value can be explained by the ultrafine microstructure and by the large quantity of intermetallics that probably formed during the PBF-LB/M process. P/S specimens showed an average microhardness of 33.9 HV0.5. This result supports what have been observed at OM. Indeed, a partial densification can explain this low microhardness values. Finally, the samples were observed using the tabletop SEM and EDX analysis was performed. SEM observation helped to gain insight into the microstructure of PBF-LB/M processed samples. Al-8Fe-4Ce produced by PBF-LB/M showed a microstructure, in which intermetallics tend to accumulate at the melt pool boundaries (MPB) due to the higher cooling rates. Moreover, the alloy is probably characterized by columnar grains as suggested by the microstructure (see Fig. 3). Columnar grain structure is common in PBF-LB/M Al alloys when there are no intermetallics or ceramic particles that can act as inoculants for the formation of equiaxial grains[18)]. EDX map (see Fig. 3) highlighted as cerium tends to be homogenously distributed in the entire microstructure while iron forms iron-rich intermetallics. Further investigation with more sophisticated techniques is required to obtain a more detailed understanding of the composition of the intermetallics.

On the other hand, P/S sample showed a completely different microstructure, with coarse intermetallics uniformly dispersed in the Al matrix (see Fig. 4). In addition, from electron backscatter diffraction (BSD) images, it is evident the presence of two types of intermetallics: one richer in iron and the other richer in cerium.

The different composition of the intermetallics seems to be confirmed by EDX analysis. Indeed, unlikely PBF-LB/M samples, here cerium rich intermetallics are clearly visible. The presence of coarsening intermetallics is mainly due to the high temperature of sintering. Indeed, although cerium and iron have low solid diffusion in aluminium, the temperature is high enough to promote coarsening even after only 1h of exposure. The addition of magnesium as sintering aid could promote sintering at lower temperatures, reducing the coarsening effect caused by the high temperature exposition[23,26)].

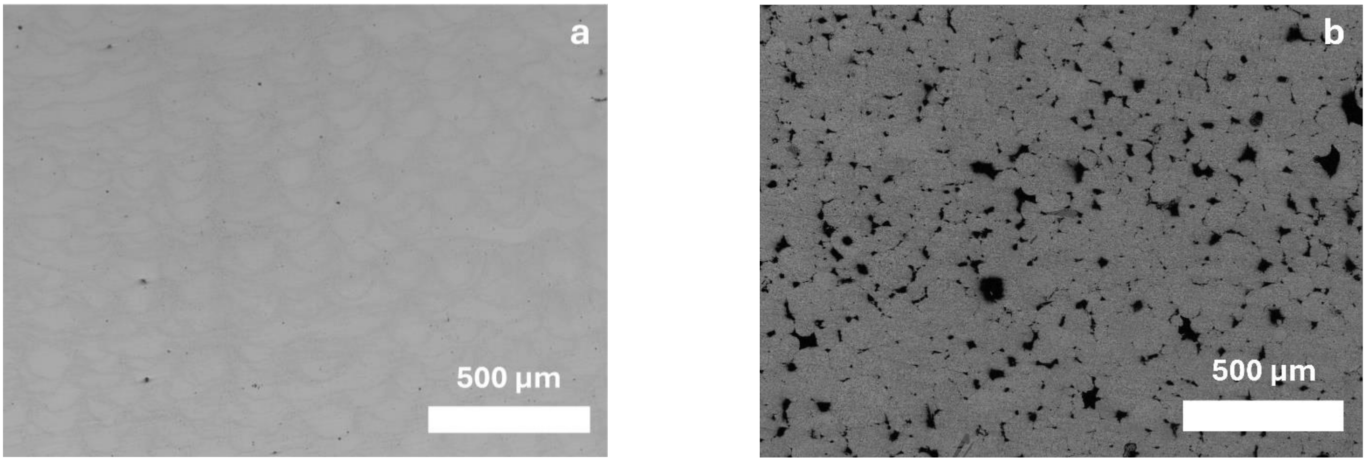

Fig.2 a) OM image of PBF-LB/M sample. b) OM image of P/S sample.

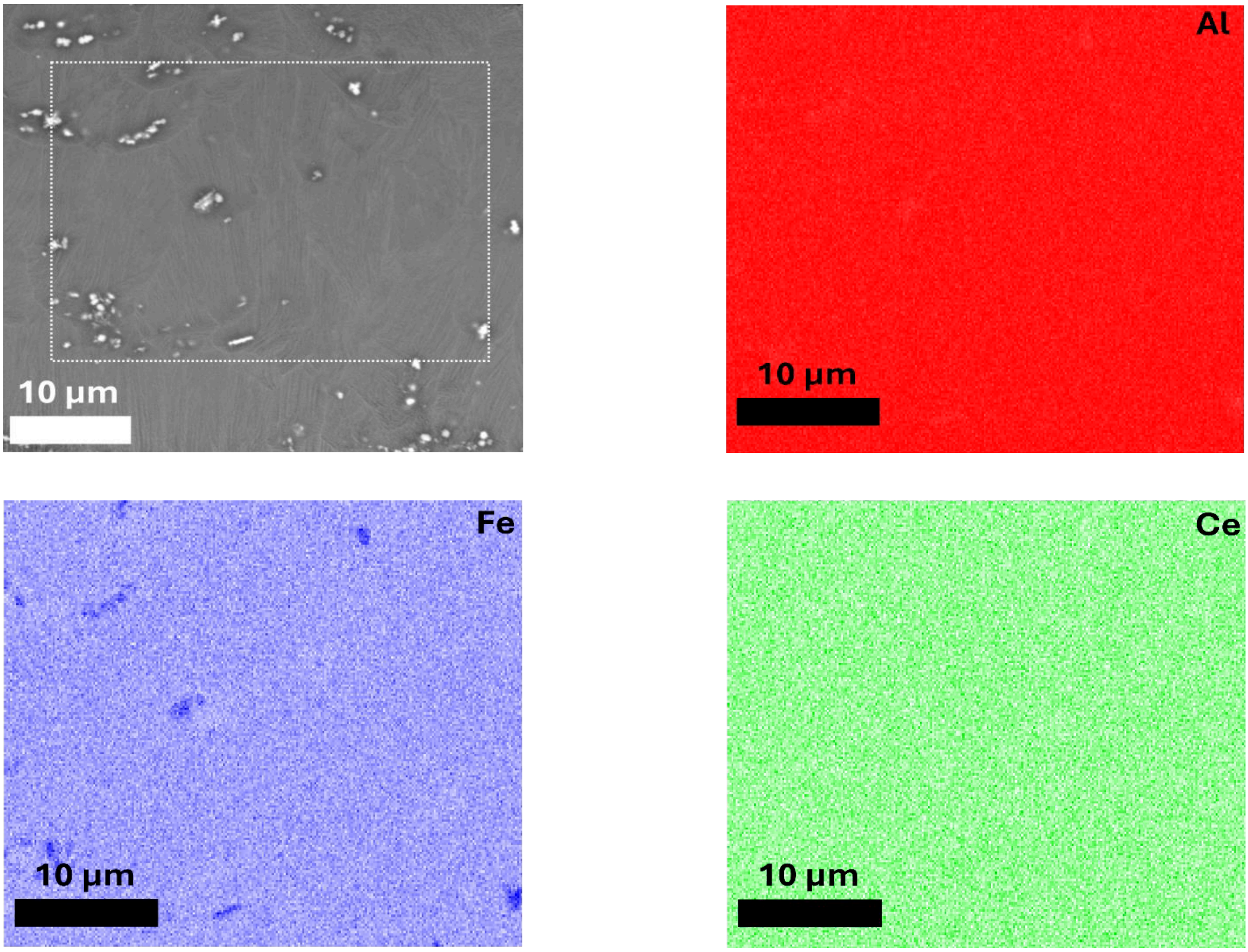

Fig. 3. BSD image of a PBF-LB/M sample with EDX map analysis.

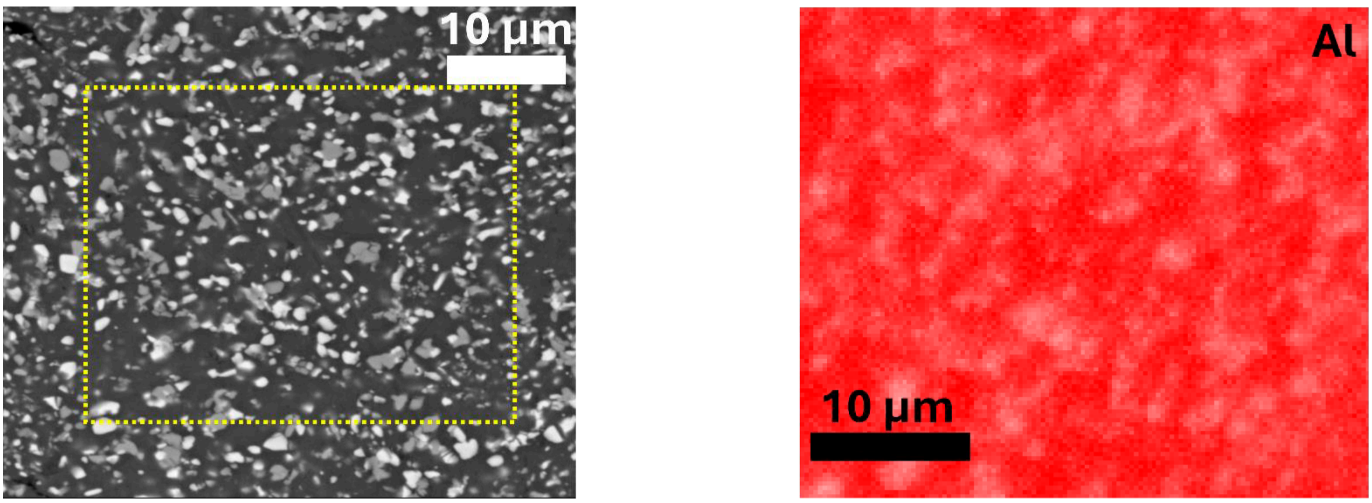

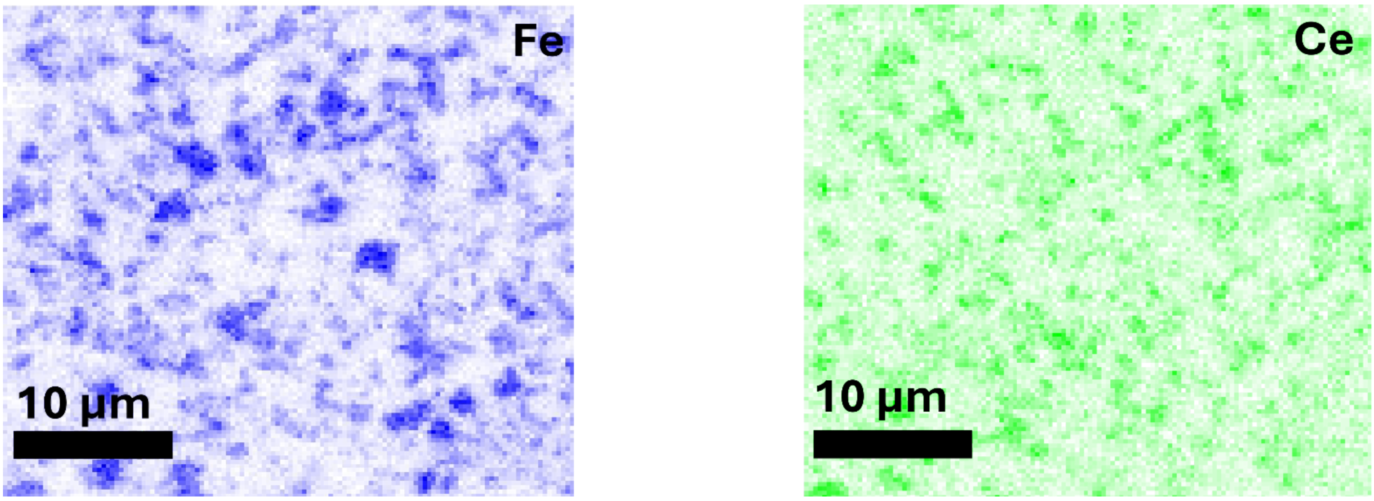

Fig. 4. BSD image of a P/S sample with EDX map analysis.

Conclusion

PBF-LB/M and P/S samples of Al-8Fe-4Ce were produced and characterized. It was demonstrated the feasibility of obtain dense and crack free specimens by PBF-LB/M with an average hardness of 179.7 HV0.5, comparable to the values of commercially established high strength AM Al alloys. The microstructural characterization shows a distribution of fine intermetallics, which have probably a composition richer in iron than in cerium. On the other hand, P/S sample did not achieve full sintering. The high sintering temperature (600 °C) combined with nitrogen atmosphere was not enough to promote sintering. This is main reason for the low hardness of the P/S specimens (average value 33.9 HV0.5). The microstructural observation highlights the presence of coarse intermetallics evenly distributed in the matrix. In addition, EDX analysis suggests the presence of both Ce and Fe rich intermetallic unlike PBF-LB/M samples. The promising results demonstrated by PBF-LB/M samples suggest a deeper microstructural investigation coupled with a full mechanical characterization. Regarding P/S process, the influence of sintering aids, such as magnesium, should be investigated in order to assess the possible use of Al-8Fe-4Ce alloy for the production of P/S components.

References

1) S. S. Li, X. Yue, Q. Y. Li, H. L. Peng, B. X. Dong, T. S. Liu, H. Y. Yang, J. Fan, S. L. Shu, F. Qiu, Q. C. Jiang, Journal of Materials Research and Technology, **27** (2023) 944-983.

2) B. Zhou, B. Liu, S. Zhang, Metals, 11 (2021) 718-746.

3) R. A. Michi, A. Plotkowski, A. Shyam, R. R. Dehoff, S. S. Babu, International Materials Reviews, **67:3** (2022) 298-345.

4) S. Bahl, K. Sisco, Yi. Yang, F. Theska, S. Primig, L. F. Allard, R. A. Michi, C. Fancher, B. Stump, R. R. Dehoff, A. Shyam, A. Plotkowski, Additive Manufacturing, **48** (2021).

5) F. Czerwinski, Materials, **13** (2020)

6) N. C. Kothari, Key Engineering Materials, **29-31** (1988) 275-290.

7) E. Bouchaud, H. Octor, T. Khan, Materials & Desing, **14** (1993) 29-32.

8) K. N. Ramakrishnan, Materials Characterization, **33** (1994) 119-128.

9) M. A. Gordillo, I. Cernatescu, T. T. Aindow, T. J. Watson, M. Aindow, Journal of Materials Science, **49** (2014) 3742–3754.

10) M. P. Moodispaw, E. Cinkilic, J. Miao, A. A. Luo, Metallurgical and Materials Transaction A, **55** (2024) 1351-1362.

11) J. C. Ekvall, R. A. Rainen, D. J. Chellman, Journal of Aircraft, **27** (1990).

12) D. l. Yaney, W. D. Nix, Metallugircal Transactions A, **18** (1987) 893-902.

13) Y. W. Kim, Dispersion Strengthened Aluminum Alloys, Y. W. Kim and W. M. Griffith ed., Phoenix, 1988, The Metallurgical Society, 1988, 157-180.

14) M. Fass, D. Eliezier, E. Aghion, F. H. Froes, Journal of Materials Science, **33** (1988) 833-837.

15) X. Yuan, X Qu, H. Yin, Z. Yan, Zhaojun Tan, Materials, **12** (2019).

16) R.W. Cooke, R.L. Hexemer Jr., I.W. Donaldson, D.P. Bishop, Journla of Materials Processing Technology, **230** (2016) 72-79.

17) P. A. Rometsch, Y. Zhu, X. Wu, A. Huang, Materials & Design, **219** (2022).

18) H.R. Kotadia, G. Gibbons, A. Das, P.D. Howes, Additive Manufacturing, **46** (2021).

19) S. Sun, L. Zhen, Y. Liu, J. Liu, H. Zhang, Journal of Materials Research, **30** (2015), 1661-1169.

20) S. J. Yu, P. Wang, H. C. Li, R. Setchi, M. W. Wu, Z. Y. Liu, Z. W. Chen, S. Waqar, L. C. Zhang, Virtual and Physical Prototyping, **18:1** (2023).
21) D. Weiss, Journals of Materials Engineering and Performance, **28** (2019) 1903-1908.
22) A. Shang, B. Stegman, D. Sinclair, X. Sheng, L. Hoppenrath, C. Shen, K. Xu, E. Flores, H. Wang, N. Chawla, X. Zhang, Journal of Materials Research and Technology, **30** (2024) 5497-5511.
23) R.N. Lumley, T.B. Sercombe, G.B. Schaffer, Metallurgical and Materials Transactions A, **30A** (1999), 457-463.
24) K. Kondoh, A. Kimura, R. Watanabe, Powder Metallurgy, **44:2** (2001), 161-164
25) A. Aversa, G. Marchese, A. Saboori, E. Bassini, D. Manfredi, S. Biamino, D. Ugues, P. Fino, M. Lombardi, Materials, **12** (2019) 1007-1025.
26) I. A. MacAskill, I. W. Donaldson, D. P. Bishop, Powder Metallurgy, **49:4** (2006), 314-322.

Received June 29, 2024; Revised September 29, 2024; Accepted October 1, 2024